

Dallas, T. and Santini, L. 2020. The influence of stochasticity, landscape structure, and species traits on abundant-centre relationships. – Ecography doi: 10.1111/ecog.05164

## <sup>561</sup> Artificial landscapes

In the main text, we describe the creation of the artificial landscapes ( $200 \times 200$  lattices) which contain population growth rates. Here, we further show how these artificial landscapes were set up with respect to step size  $\beta$  (Figure A1) and the amount of environmental noise  $\eta$  (Figure A2) in the spatial distribution of population growth rates.

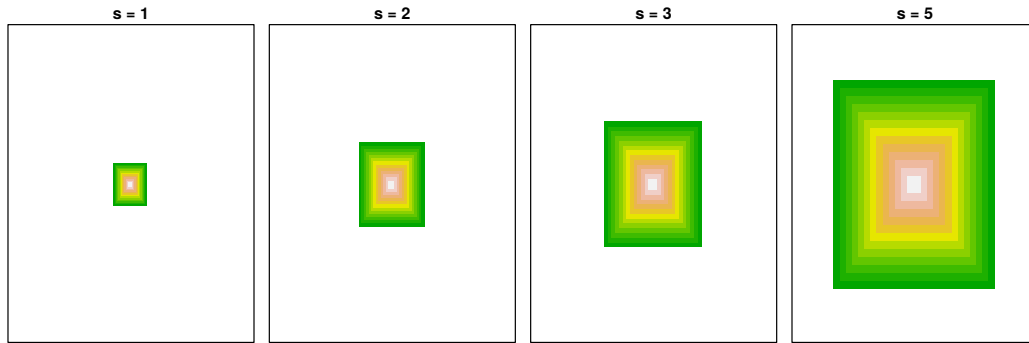


Figure A1. Step size ( $\beta$ ) controlled both the size and the gradient of species population growth rates on the landscape. Larger values of  $\beta$  correspond to larger and more gradually changing population growth rates. The default value used in the simulation analyses was 5.

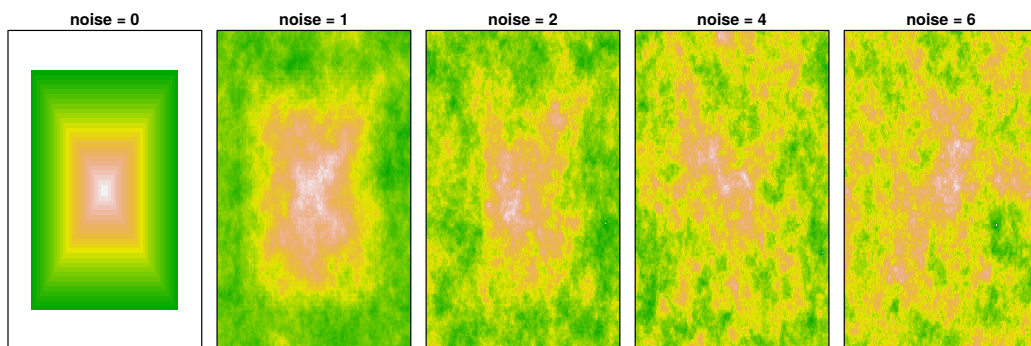


Figure A2. Environmental noise ( $\eta$ ) controlled the amount of spatially-autocorrelated noise was included in the linear gradient of population growth rates (seen in the first panel, where  $\eta = 0$ ). The default value used in the simulation analyses was 1.

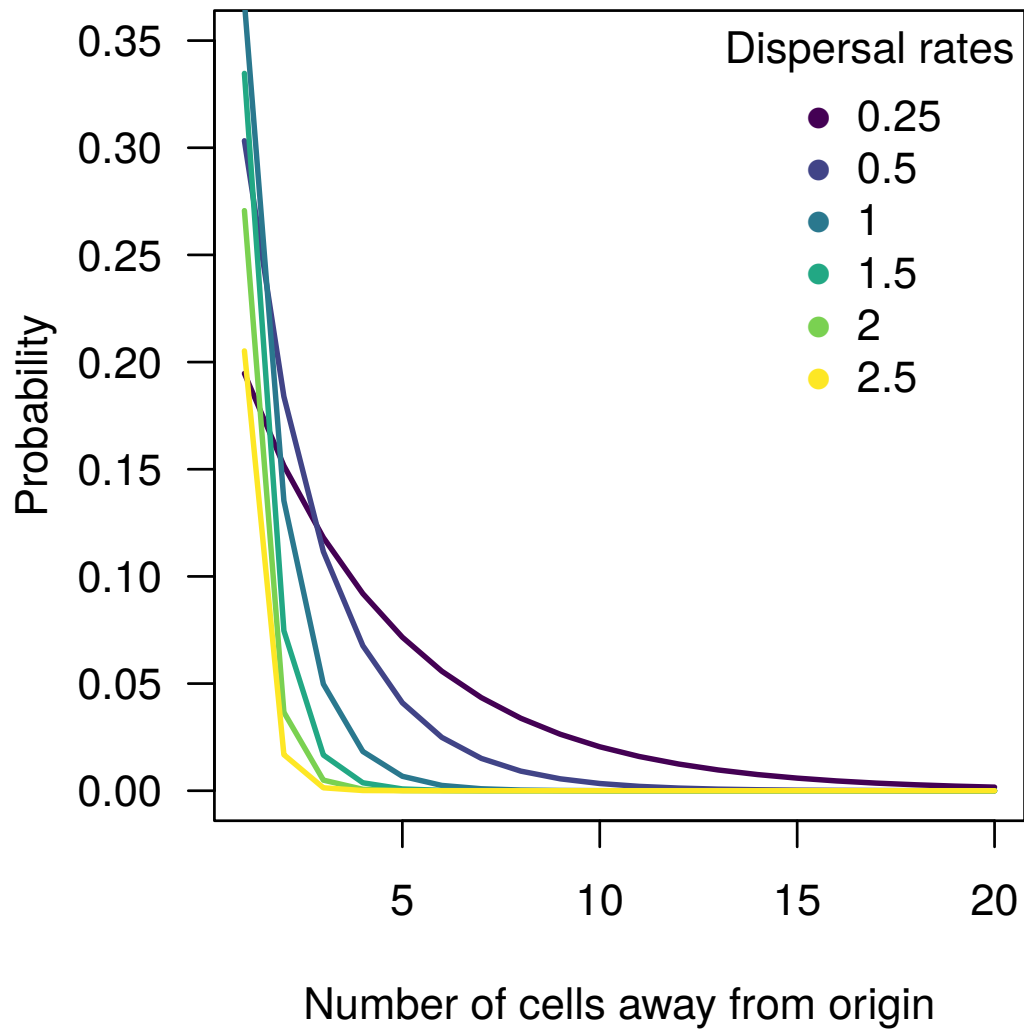


Figure A3. Dispersal kernel shape was determined by the rate parameter  $\gamma$ . We selected  $\gamma$  values across a wide range, representing a diverse range of dispersal kernels.

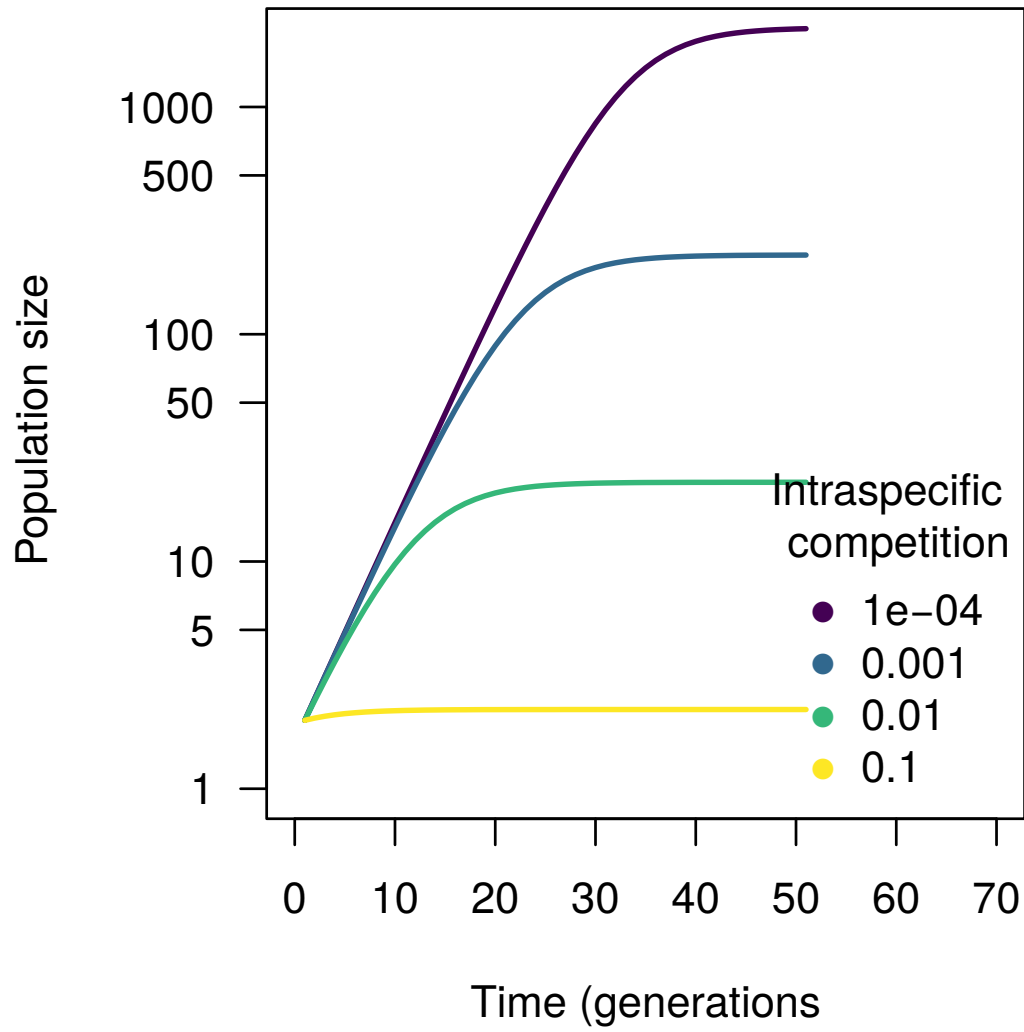


Figure A4. Starting with an initial population size of  $N_t=2$  and population growth rate ( $R_n = 1.25$ ), intraspecific competition ( $\alpha$ ) determines the equilibrial population dynamics in the deterministic Ricker model.



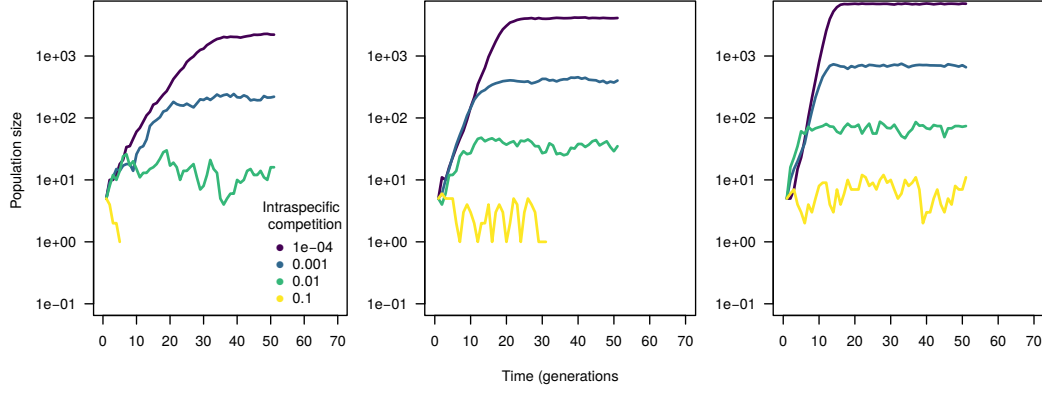


Figure A5. Building on the deterministic Ricker model, we examine one realization of the stochastic model for each combination of population growth rate  $R_n$  (1.25, 1.5, 2, from left to right) and intraspecific competition coefficient ( $\alpha$ ), starting with a population of 5 individuals. When competition is very high, populations tended to go extinct (yellow line in the left panel), but persist longer when population growth rate is high enough to counteract the strong competitive effects.

## 567 Relationship between geographic and niche distance

568 In simulated landscapes with environmental noise, the location of geographic and  
569 niche centers can differ substantially. This is especially true as we increase the  
570 amount of environmental noise ( $\eta$ ) in the landscape. We examine this by looking at  
571 the correlations between the geographic distance to the range center (geographic)  
572 and distance in niche space (simply the 1-dimensional distance between max pop-  
573 ulation growth and a given cell's value). We measured the relationship between 574  
geographic and niche distance for each simulated landscape at three different time  
75 points (50, 250, and 500 generations). The vast majority of correlations were pos-  
576 itive, but varied greatly (Figure A6). Whether this relationship holds in natural  
577 system is a quite different question.

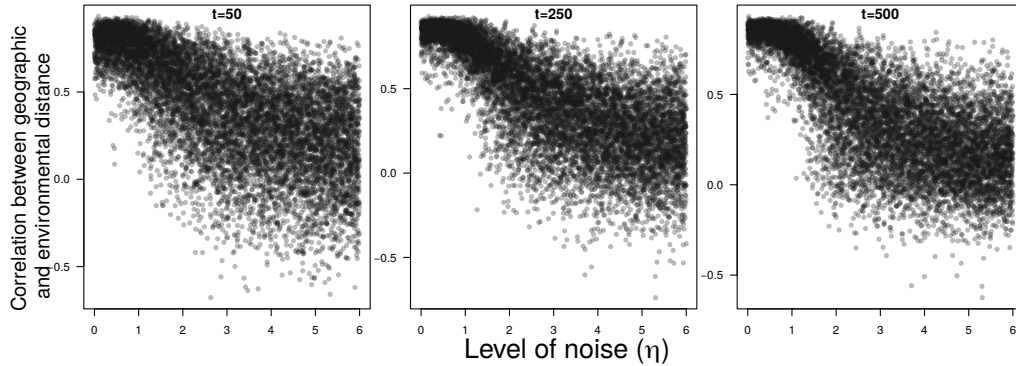


Figure A6. The relationship between distance in geographic space and distance in niche space for each simulated landscape at 50, 250, and 500 generations (corresponding to the different panels), and how this correlation was influenced by the amount of environmental noise ( $\eta$ ). We demonstrate a clear decoupling of the relationship between geographic and environmental distance with increasing environmental noise  $\eta$ .

578 **The effect of the number of generations considered on abundant-**  
579 **centre relationships**

Population sizes are variable through time, such that the deterministic assumption of asymptotic approach to carrying capacity (e.g. our deterministic Ricker model) is ridiculous. We report results after 50 generations in the main text, but also provide plots for both deterministic and stochastic formulations of the Ricker model at 250 and 500 generations. This is also inherently a gross oversimplification, as we are naturally assuming that demographic parameters and landscape structure are remaining fixed this entire time, such that dispersal is the only thing limiting population size in the deterministic model. We find similar results at 250 and 500 generations relative to the 50 generation timeline in the main text (Figure A7 -A14).

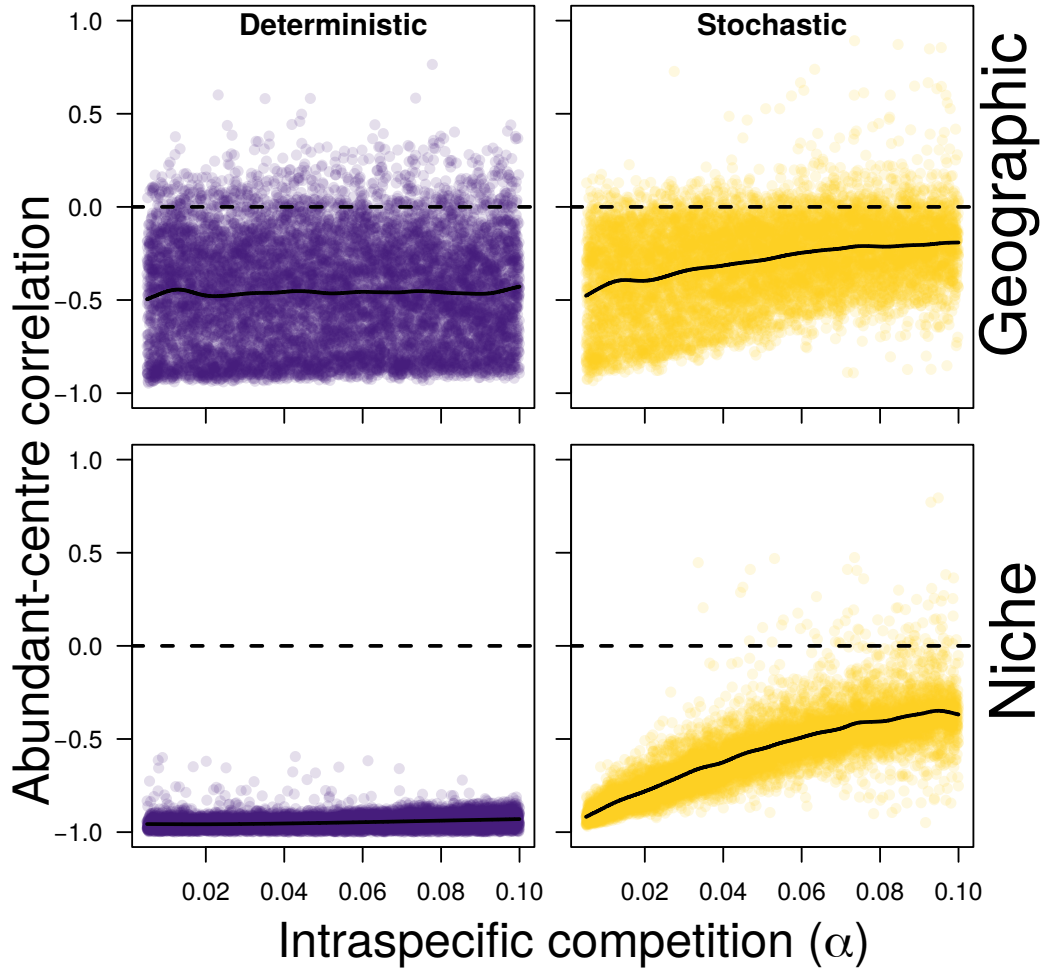


Figure A7. Abundant-centre relationships – quantified using Spearman’s rank correlations – in geographic space (top row) and niche space (bottom row) and in a deterministic model (left column) and a stochastic model (right column) at 250 generations. Abundant centre relationships in geographic space were especially susceptible to intraspecific competition ( $\alpha$ ), though incorporating a small degree of stochasticity caused intraspecific competition to strongly affect evidence for abundant centre relationships in geographic and niche space. Smoothed splines are plotted to show the general trends.

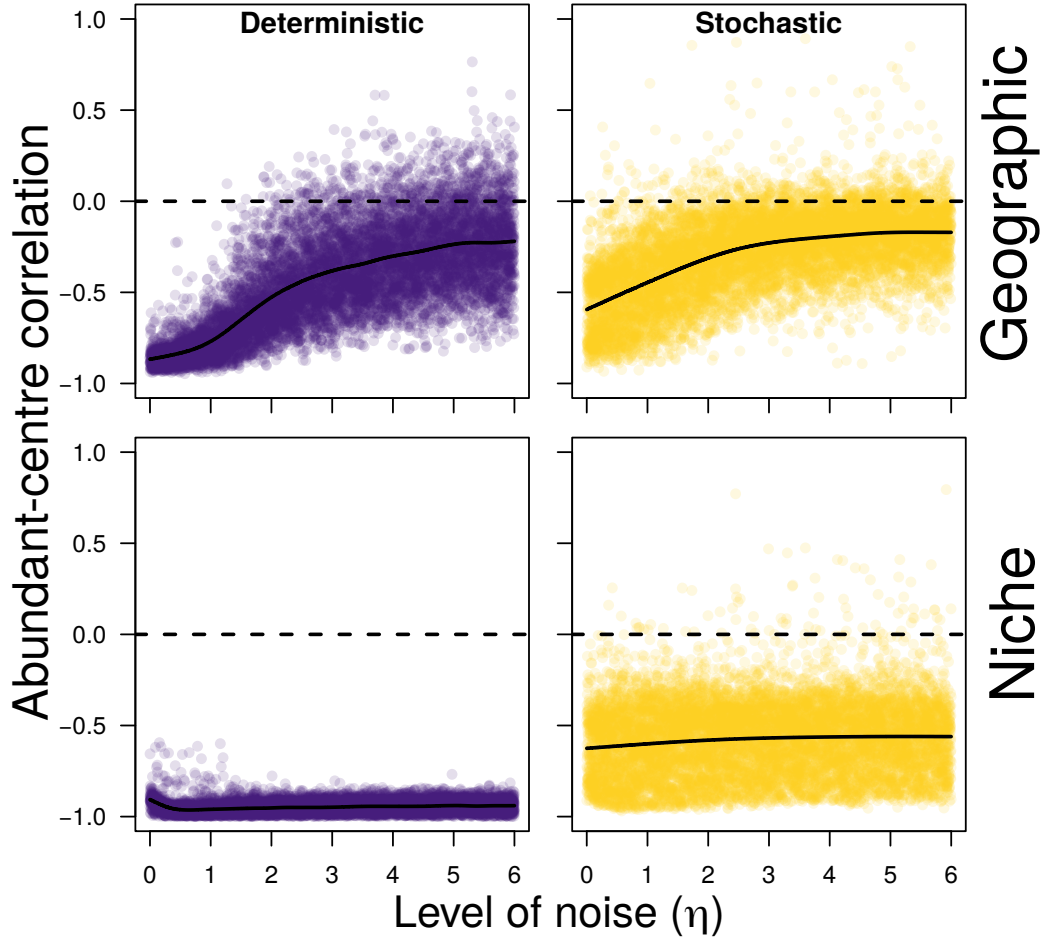


Figure A8. A realistic amount of environmental variation ( $\eta$ ) – overlaid on the artificial relationship imposed between species geographic location, niche limits and rate of population growth – reduced evidence for abundant centre relationships strongly in geographic space at 250 generations. Abundant centre relationships – quantified as Spearman’s rank correlations – in terms of niche position were relatively unaffected by this variation, but were sensitive to very small amounts of demographic stochasticity (lower right panel). Smoothed splines are plotted to show the general trends.

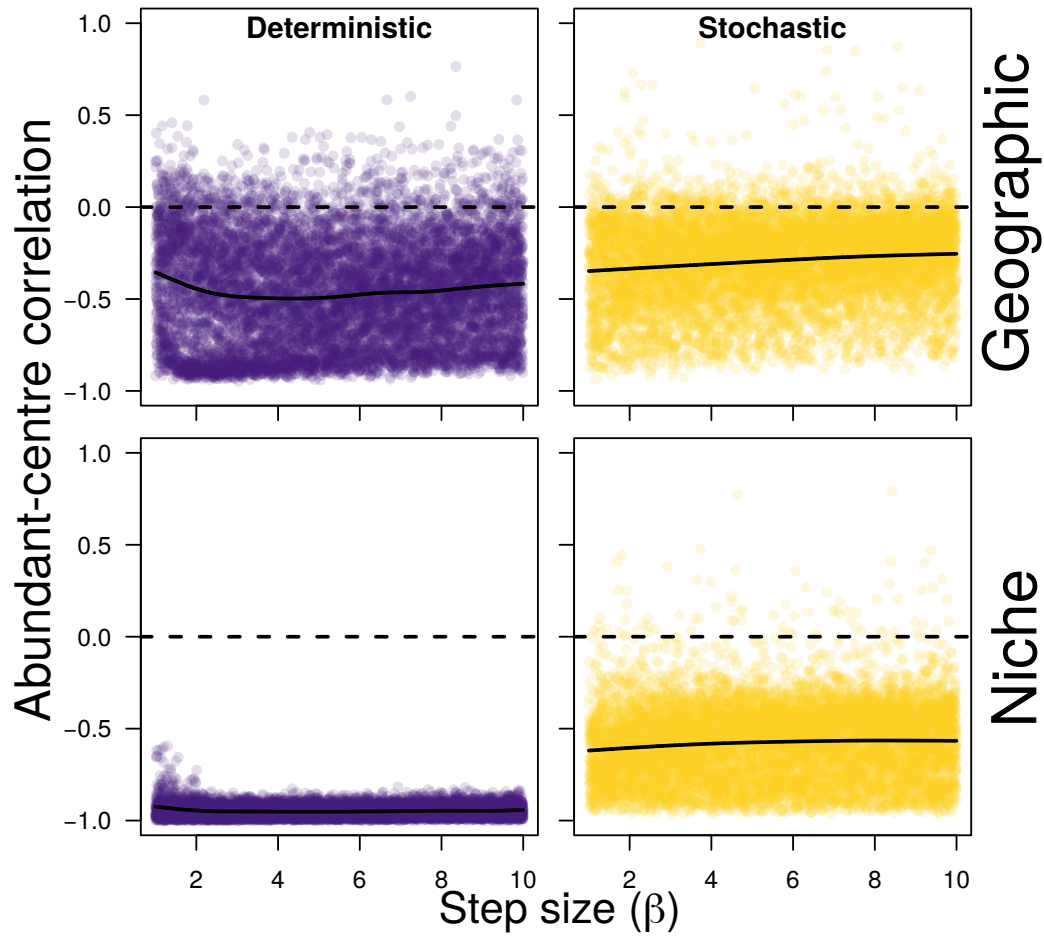


Figure A9. The rate of change in population growth rates across the artificial landscapes ( $\beta$ ) reduced evidence for abundant centre relationships – quantified as Spearman’s rank correlations – in geographic space for both deterministic and stochastic model formulations at 250 generations. In the deterministic model, an abundant-centre in niche space is inevitable as a function of the simulation design. Smoothed splines are plotted to show the general trends.

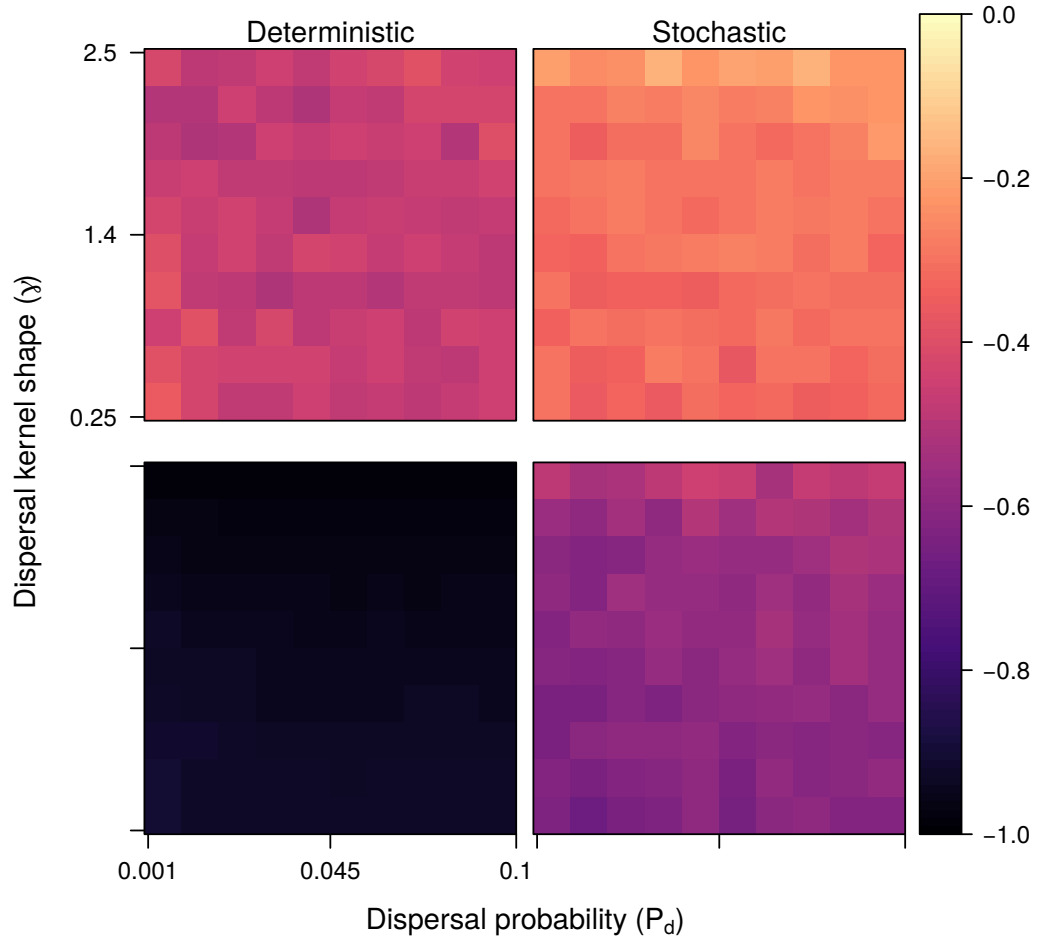


Figure A10. The joint effects of dispersal probability ( $P_d$ ; x-axis) and dispersal kernel shape parameter ( $\gamma$ ) on abundant-centre relationship strength (color scale) in geographic space (top row) and niche space (bottom row) for both the deterministic (left column) and stochastic (right column) model formulations at 250 generations. All relationships were negative on average, and dispersal probability and distance did not appear to strongly influence resulting abundant-centre patterns in our simulations.

500 generations



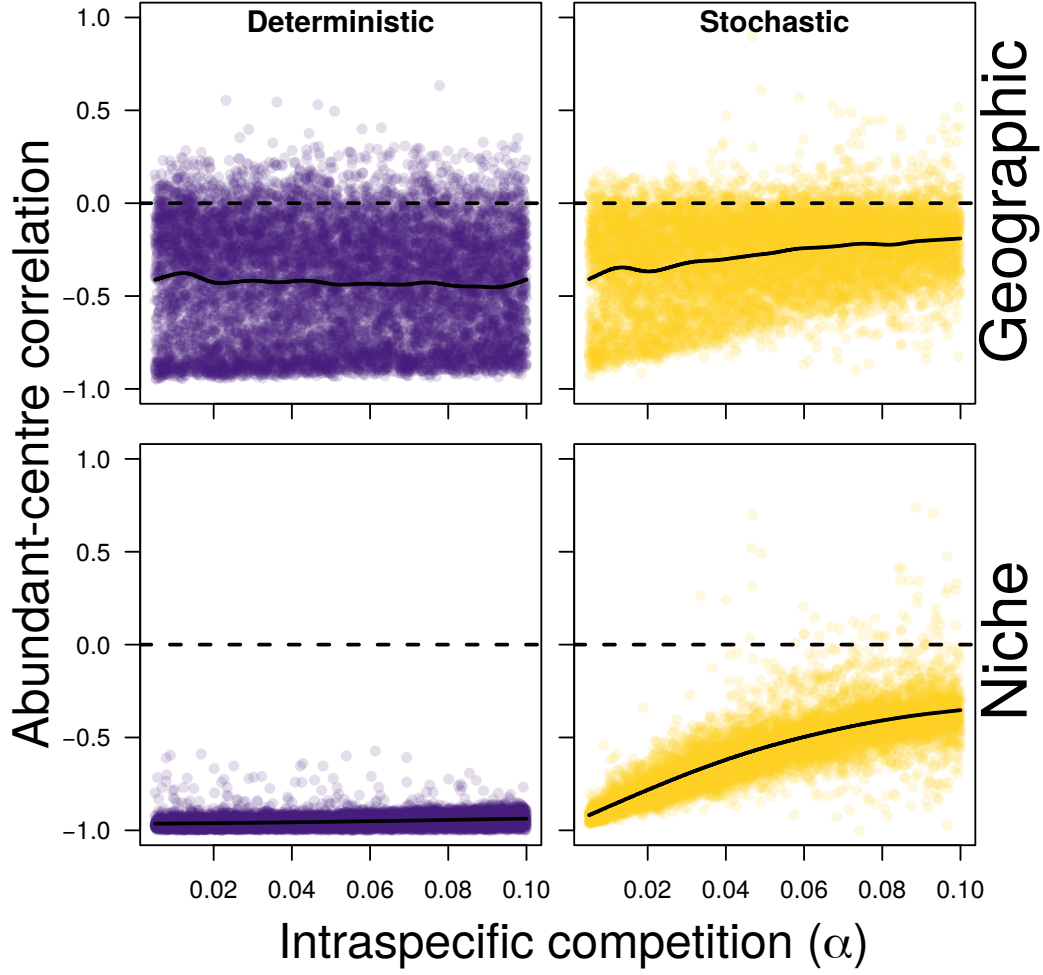


Figure A11. Abundant-centre relationships – quantified using Spearman’s rank correlations – in geographic space (top row) and niche space (bottom row) and in a deterministic model (left column) and a stochastic model (right column) at 500 generations. Abundant centre relationships in geographic space were especially susceptible to intraspecific competition ( $\alpha$ ), though incorporating a small degree of stochasticity caused intraspecific competition to strongly affect evidence for abundant centre relationships in geographic and niche space. Smoothed splines are plotted to show the general trends.

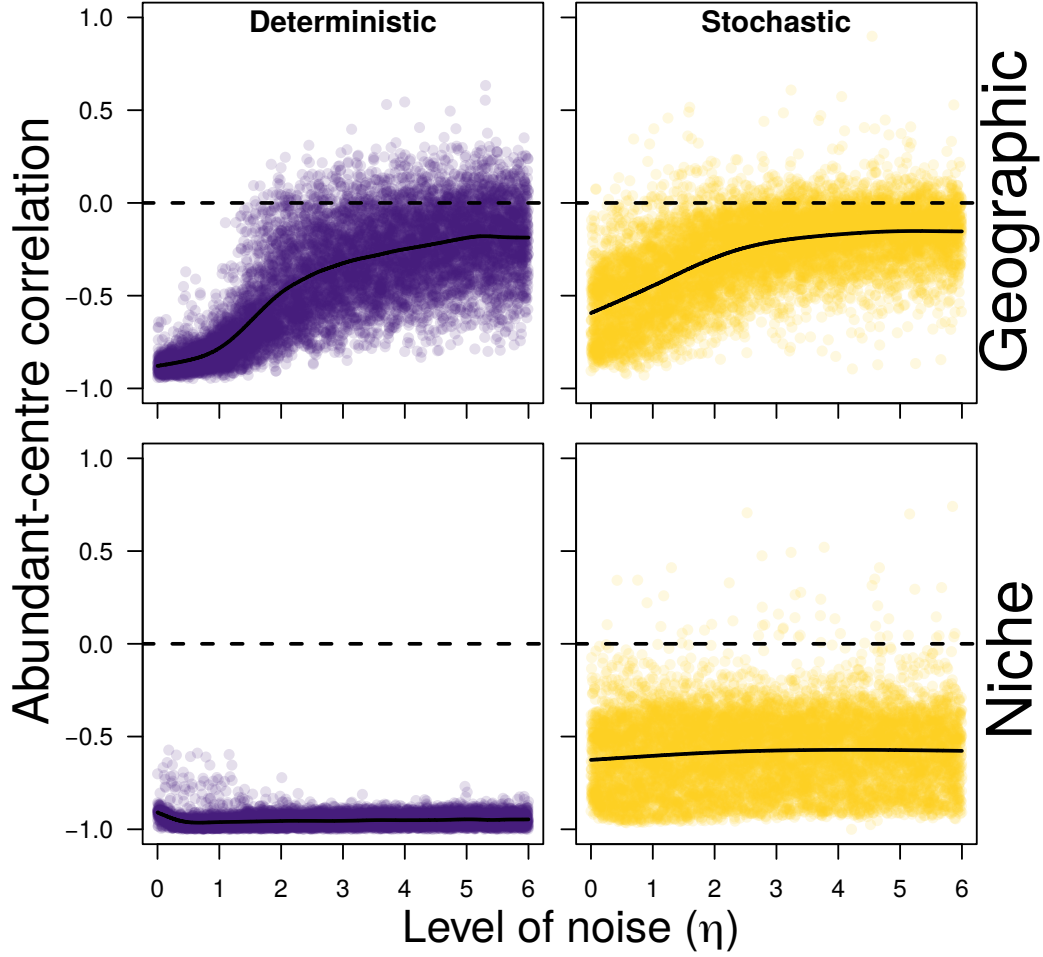


Figure A12. A realistic amount of environmental variation ( $\eta$ ) – overlaid on the artificial relationship imposed between species geographic location, niche limits and rate of population growth – reduced evidence for abundant centre relationships strongly in geographic space at 500 generations. Abundant centre relationships – quantified as Spearman’s rank correlations – in terms of niche position were relatively unaffected by this variation, but were sensitive to very small amounts of demographic stochasticity (lower right panel). Smoothed splines are plotted to show the general trends.

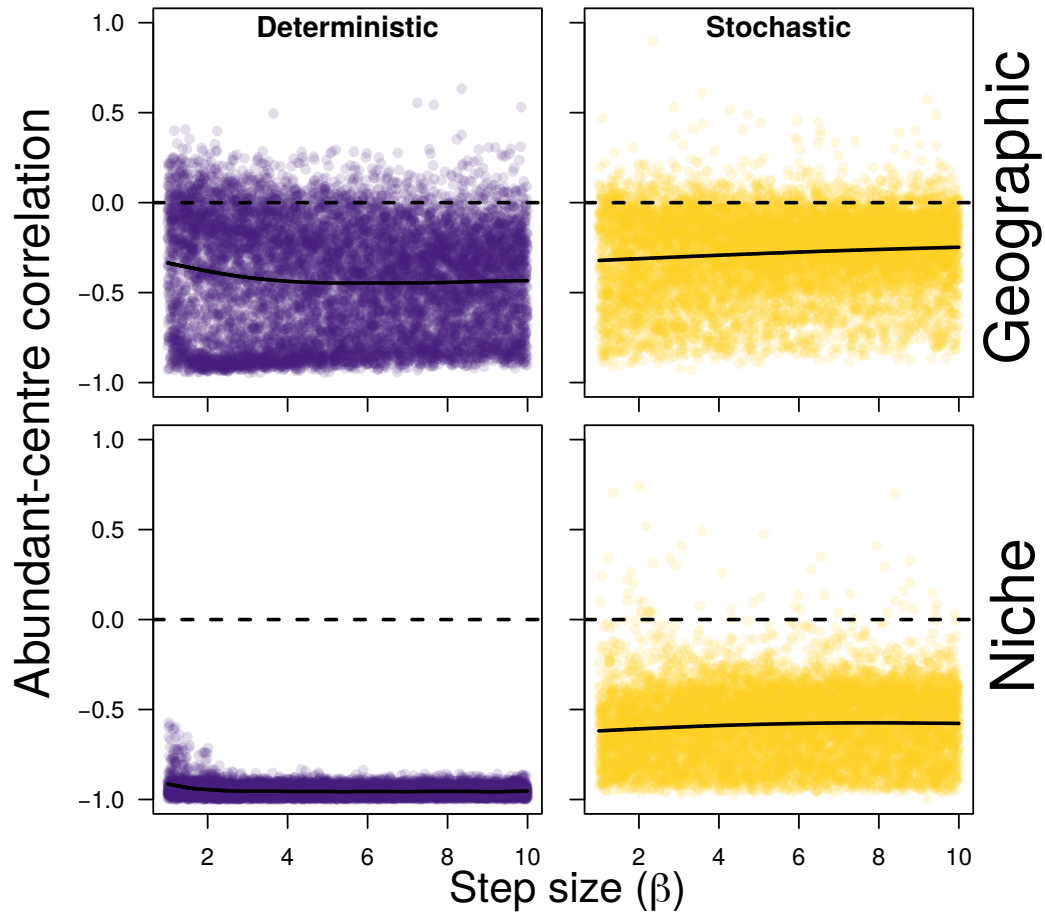


Figure A13. The rate of change in population growth rates across the artificial landscapes ( $\beta$ ) reduced evidence for abundant centre relationships – quantified as Spearman’s rank correlations – in geographic space for both deterministic and stochastic model formulations at 500 generations. In the deterministic model, an abundant-centre in niche space is inevitable as a function of the simulation design. Smoothed splines are plotted to show the general trends.

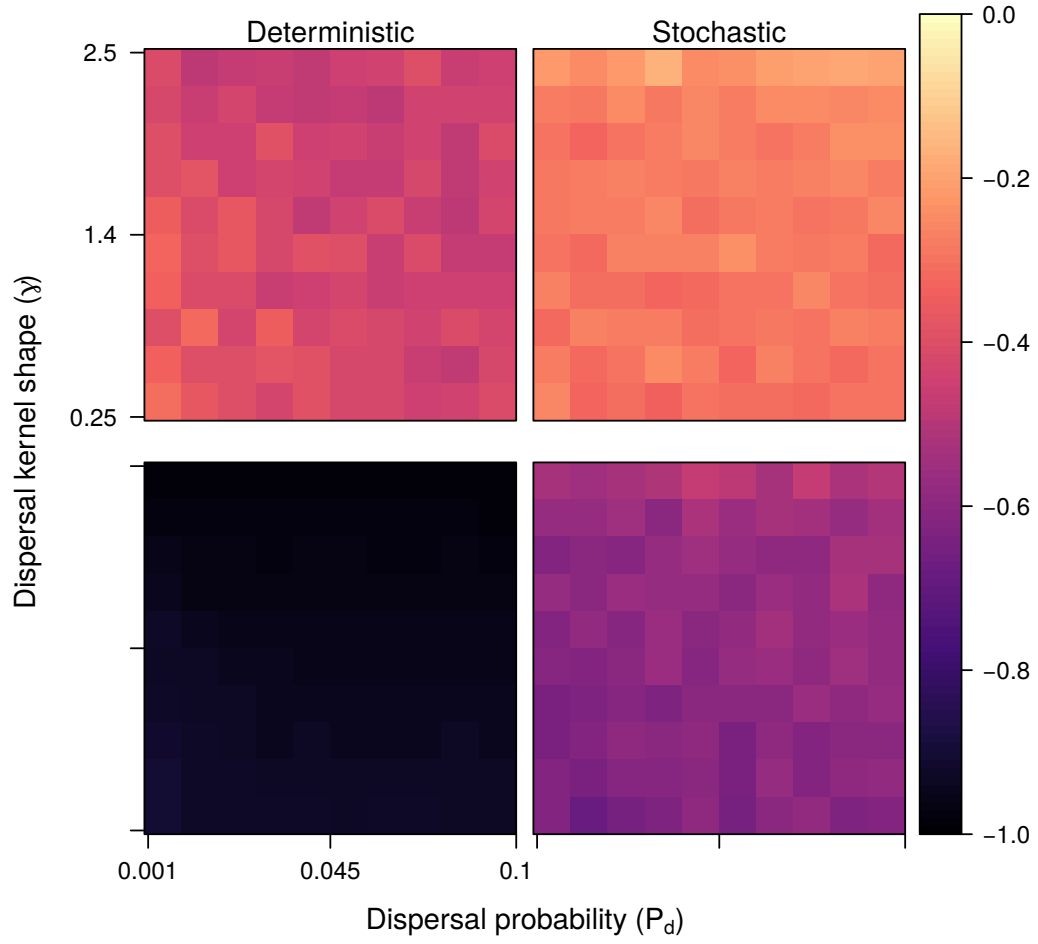


Figure A14. The joint effects of dispersal probability ( $P_d$ ; x-axis) and dispersal kernel shape parameter ( $\gamma$ ) on abundant-centre relationship strength (color scale) in geographic space (top row) and niche space (bottom row) for both the deterministic (left column) and stochastic (right column) model formulations at 500 generations. All relationships were negative on average, and dispersal probability and distance did not appear to strongly influence resulting abundant-centre patterns in our simulations.

## 591 **Simulating landscapes with fixed parameter values**

592 We examined five levels for each parameter across a wide range of values, and  
593 simulated species spatial population dynamics 10 times for each level. This allows  
594 us to tease apart the influence of each parameter while holding the others constant.  
595 For this set of simulations, we also examined the temporal variation in abundant  
596 centre relationship slope, finding unrealistically little variation in the deterministic  
597 model, and strikingly high variation in the stochastic model (Figure A19 - A26).

598 For each simulation and at each timestep, we calculated Spearman's rank corre-  
599 lations between population abundance in each cell and *a*) the Euclidean distance  
600 between the geographic range centre (which corresponds to the area of highest  
601 population growth rate), and *b*) the difference of population growth rates from  
602 the maximum. This first relationship addresses the abundant centre relationship  
603 in terms of distance from the geographic range centre of the species. The second  
604 relationship is a simplified way to address distance from niche centre, making the  
605 implicit assumption that the highest value population growth rate corresponds to  
606 the centre of the niche. We further assume that this niche axis is directly propor-  
607 tional to population growth rate.

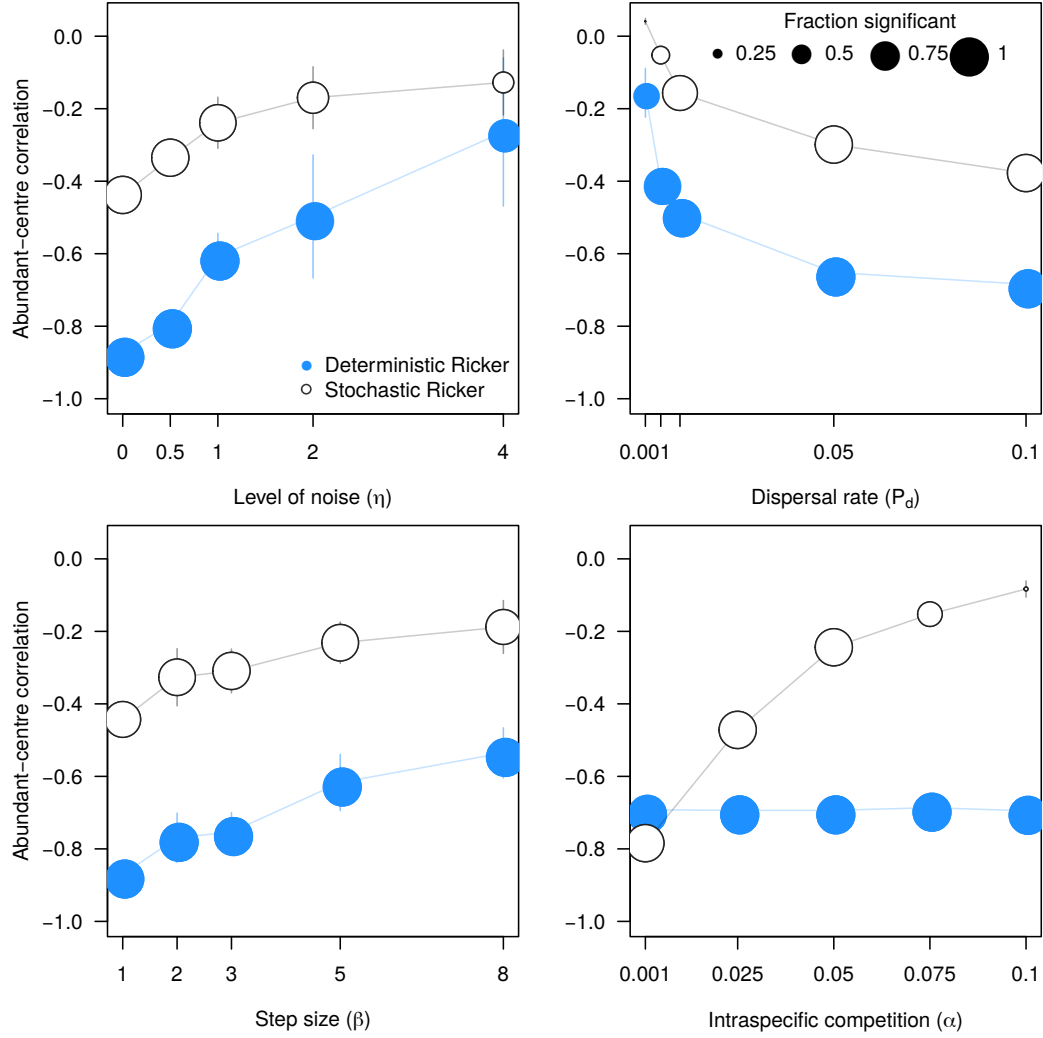


Figure A15. Abundant-centre relationships in geographic space – quantified using Spearman’s rank correlations – were sensitive to model parameterization and incorporation of demographic stochasticity. More gradual and larger species ranges tended to weaken abundant-centre relationships, as did increasing environmental noise ( $\eta$ ), increasing intraspecific competition in the stochastic model ( $\alpha$ ), and decreasing dispersal probability ( $P_d$ ). Point size is proportional to the fraction of correlation coefficients that were significant. Error bars are standard deviations across the 10 simulations per treatment level.

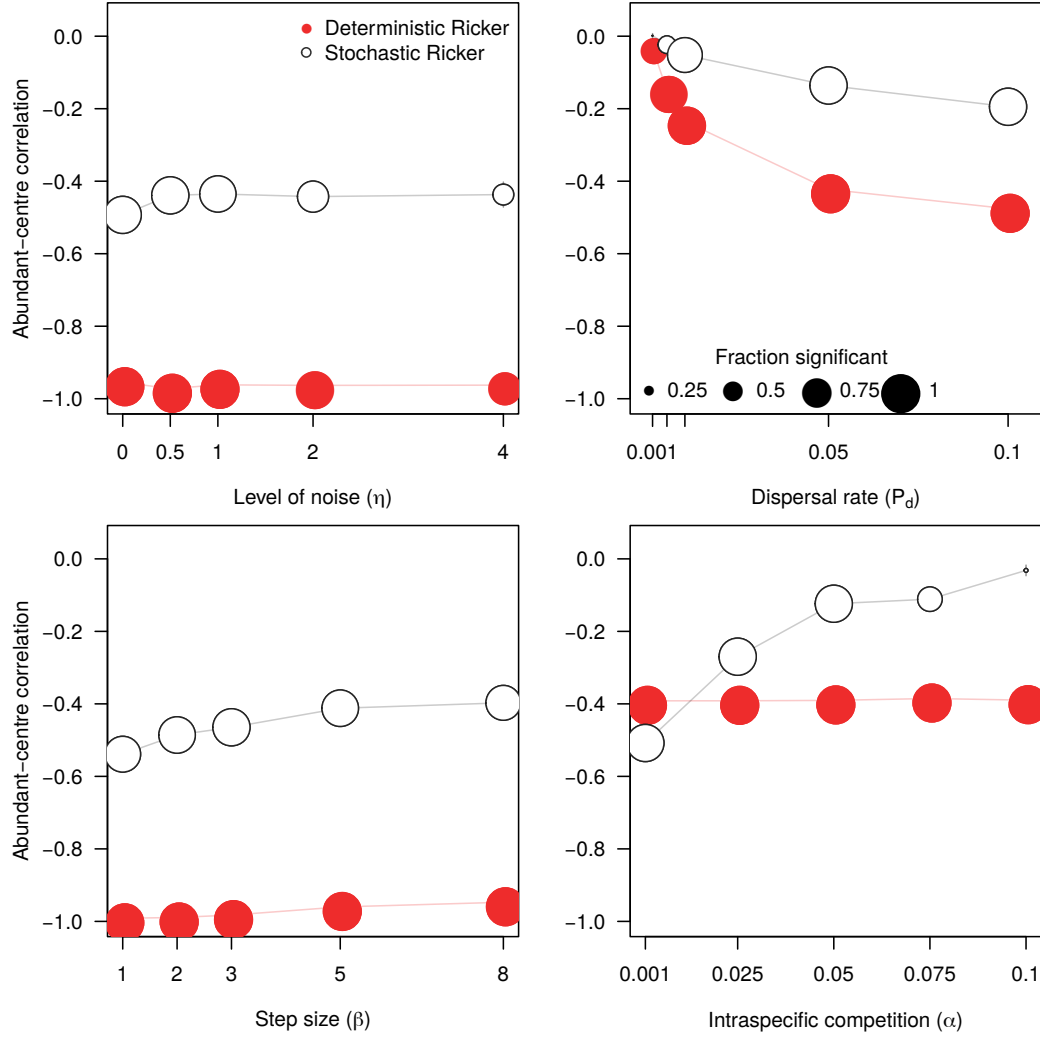


Figure A16. Abundant-centre relationships in niche space – quantified using Spearman’s rank correlations – were sensitive to model parameterization and incorporation of demographic stochasticity. Deterministic models suggested that abundant-centre relationships in one-dimensional niche space – quantified as the difference between each growth rate from maximum – were insensitive to changing parameters (except for dispersal rate  $P_d$ ). However, models incorporating demographic stochasticity estimated much weaker abundant-centre relationships, and demonstrated a clear influence of intraspecific competition ( $\alpha$ ) and dispersal rate ( $P_d$ ). Point size is proportional to the fraction of correlation coefficients that were significant. Error bars are standard deviations across the 10 simulations per treatment level.

## 608 **Insensitivity to distance measure used**

609 The measure used to estimate distance from the centre of a species geographic  
610 range or climatic niche may influence the resulting support for the abundant-  
611 centre hypothesis (Osorio-Olvera et al., 2019). For completeness, we also estimated  
612 distance using Mahalanobis distance instead of Euclidean distance as in the main  
613 text. Mahalanobis distance benefits from directly incorporating the covariance  
614 structure between geographic or niche axes. Given the strong amount of covariance  
615 in geographic space in our simulated landscapes, we might expect Mahalanobis  
616 distance to yield stronger support for abundant-centre relationships. It does not  
617 (Figure A17), perhaps because of the close association between the two distance  
618 measures (Figure A18).



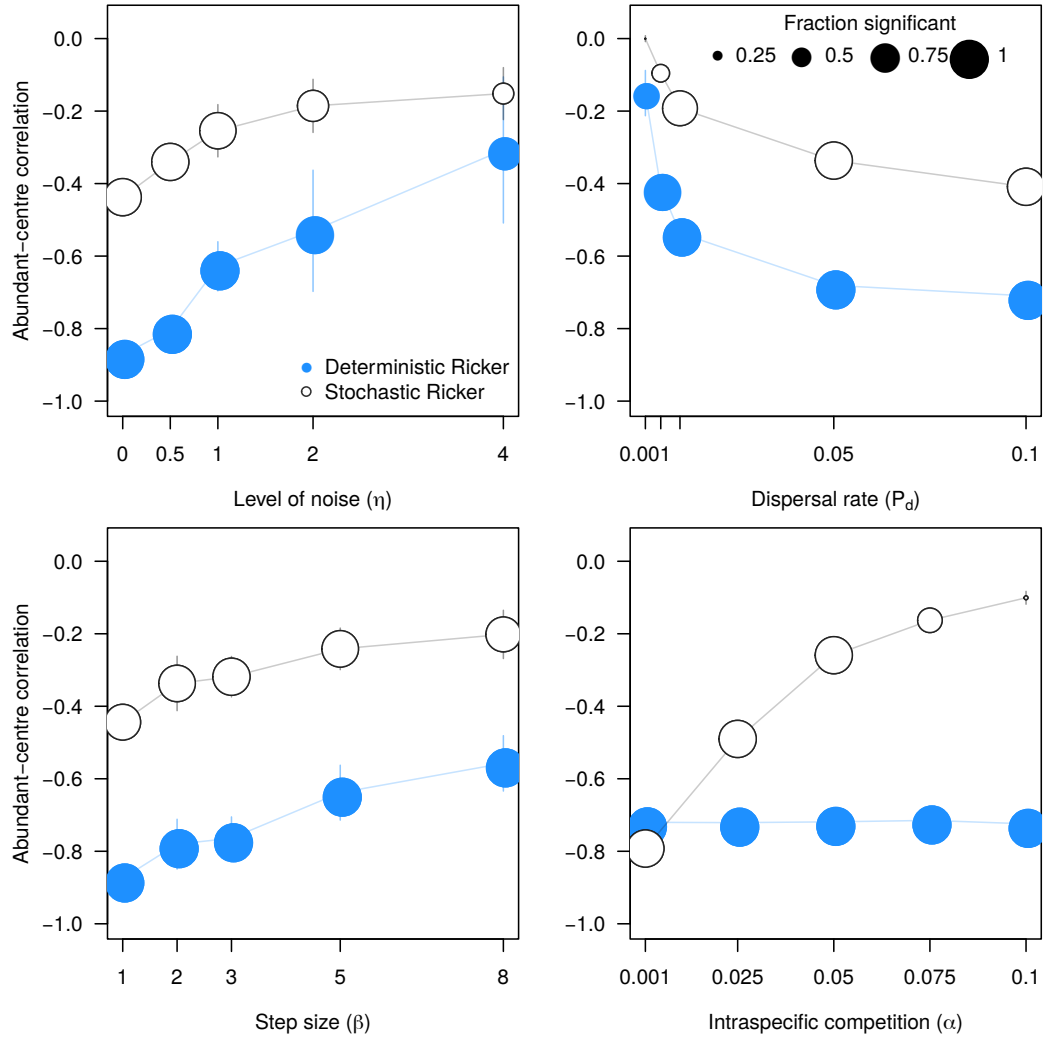


Figure A17. Using Mahalanobis distance instead of Euclidean distance did not influence results of deterministic or stochastic model simulations. Point size is proportional to the fraction of correlation coefficients that were significant. Error bars are standard deviations across the 10 simulations per treatment level.

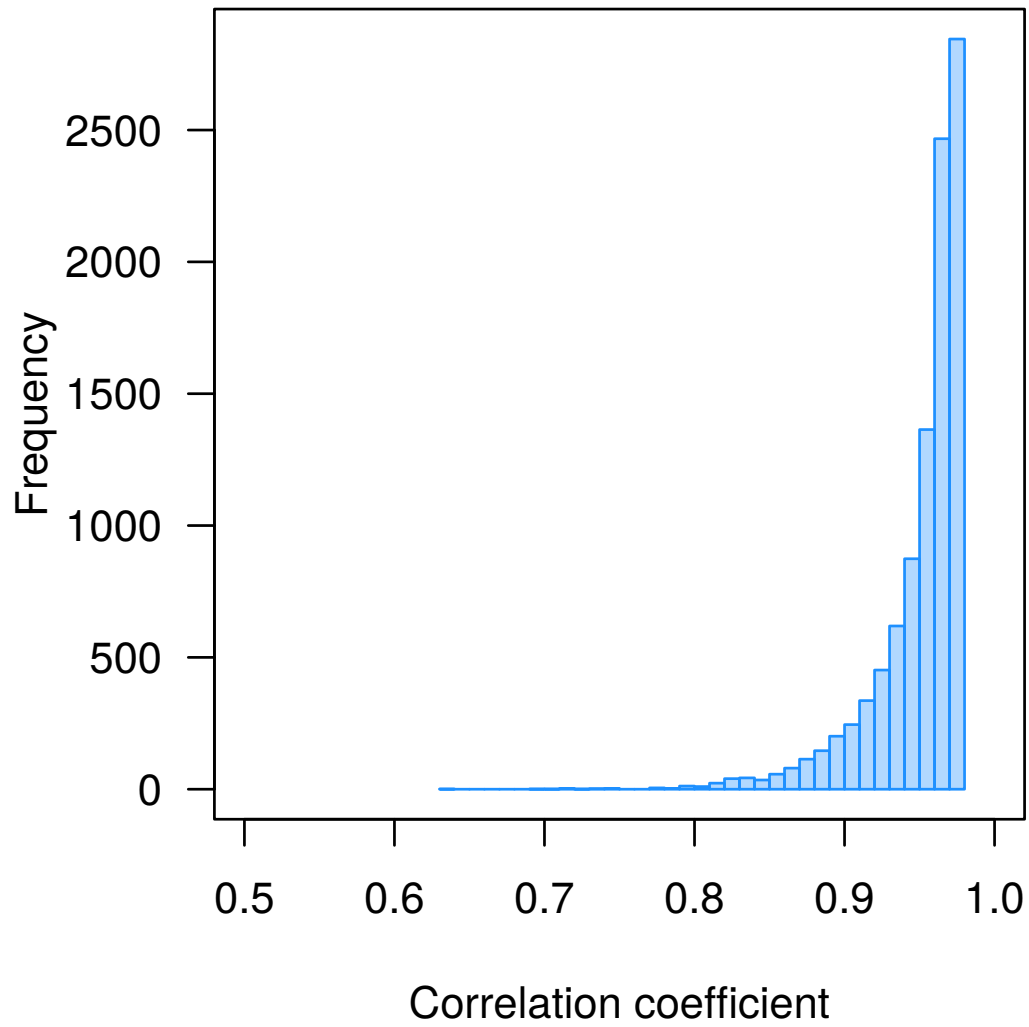


Figure A18. The distribution of Pearson's correlation coefficients between Euclidean and Mahalanobis distance from the geographic range center of the simulated landscapes. The mean correlation coefficient was 0.95.

## 619 **Time series plots**

Simulations were initiated with species not at their equilibrial populations for each cell. To examine how the transient dynamics of spreading populations influences abundant-centre correlations, we visualized time series of abundant-centre relationships measured in geographic (Figure A19 - A22) and climatic niche (Figure 23 - A26) space. We find a large degree of variability in abundant-centre support in the stochastic model, while we generally see a smooth non-linear decline in abundant-centre slope in the deterministic model simulations.

## Geographic space

627

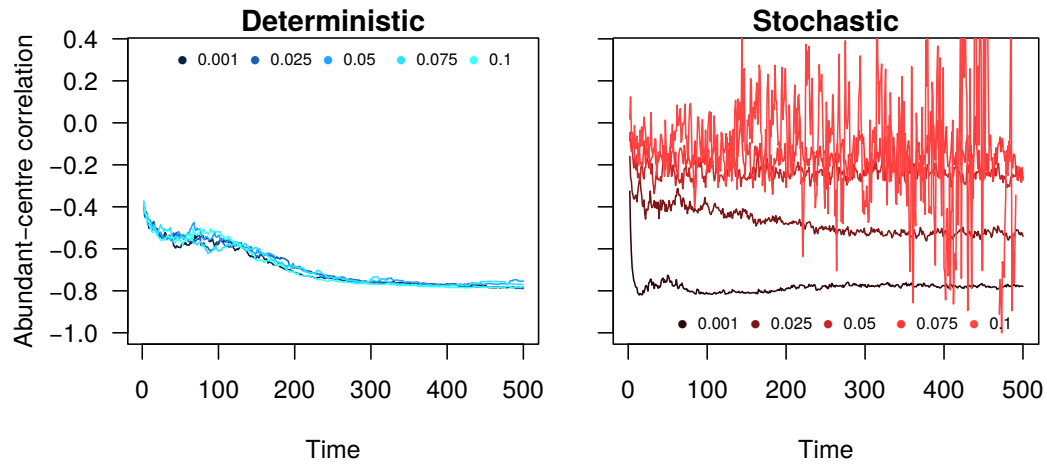


Figure A19. A representative simulation of abundant-centre relationships in geographic space over the course of the 500 timestep simulation for both deterministic (left panel) and stochastic (right panel) model, examining the influence of intraspecific competition  $\alpha$ .

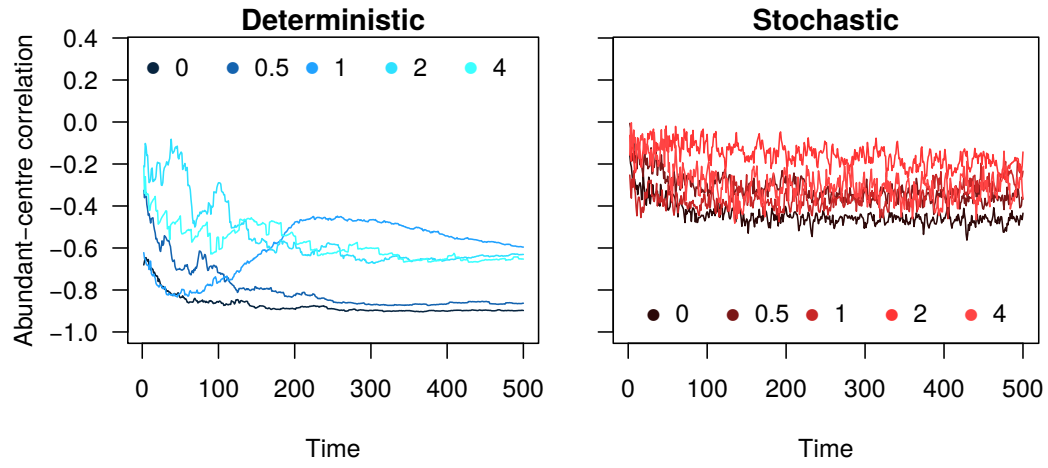


Figure A20. A representative simulation of abundant-centre relationships in geographic space over the course of the 500 timestep simulation for both deterministic (left panel) and stochastic (right panel) model, examining the influence of environmental noise  $\eta$ .

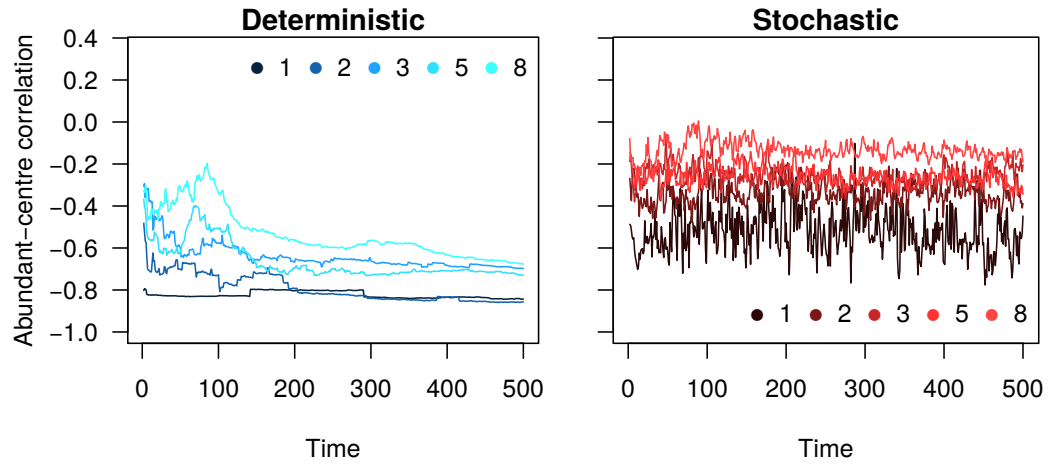


Figure A21. A representative simulation of abundant-centre relationships in geographic space over the course of the 500 timestep simulation for both deterministic (left panel) and stochastic (right panel) model, examining the influence of step size  $\beta$ .

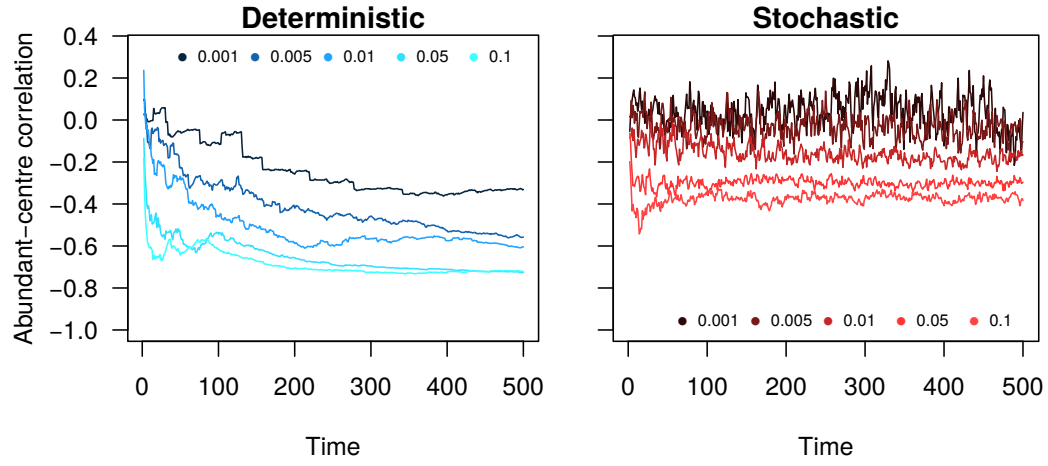


Figure A22. A representative simulation of abundant-centre relationships in geographic space over the course of the 500 timestep simulation for both deterministic (left panel) and stochastic (right panel) model, examining the influence of dispersal probability  $P_d$ .

# Niche space

628

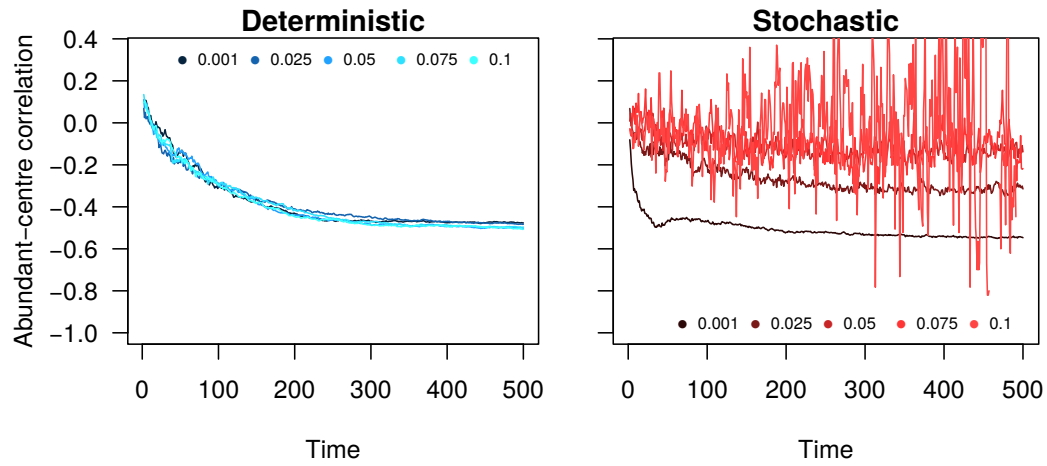


Figure A23. A representative simulation of abundant-centre relationships in climatic niche space – defined in a single dimension corresponding to population growth rates – over the course of the 500 timestep simulation for both deterministic (left panel) and stochastic (right panel) model, examining the influence of intraspecific competition  $\alpha$ .



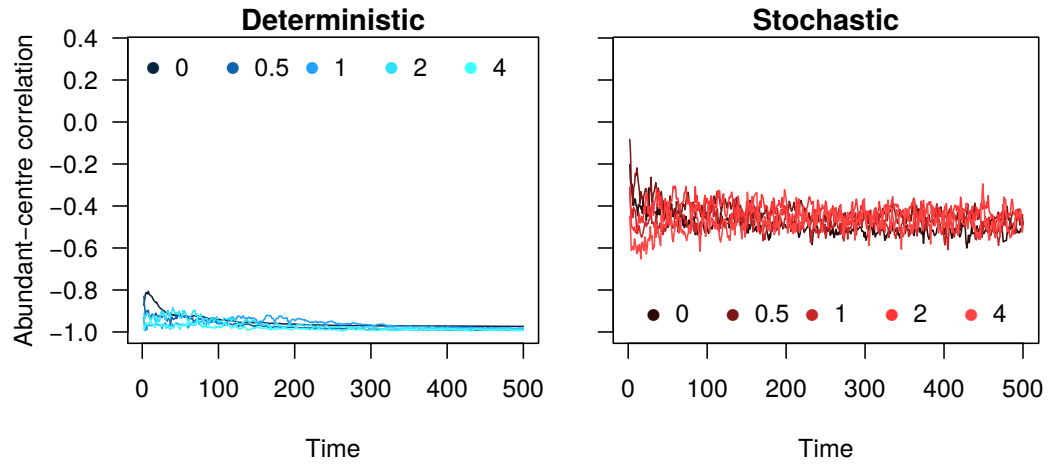


Figure A24. A representative simulation of abundant-centre relationships in climatic niche space – defined in a single dimension corresponding to population growth rates – over the course of the 500 timestep simulation for both deterministic (left panel) and stochastic (right panel) model, examining the influence of environmental noise  $\eta$ .

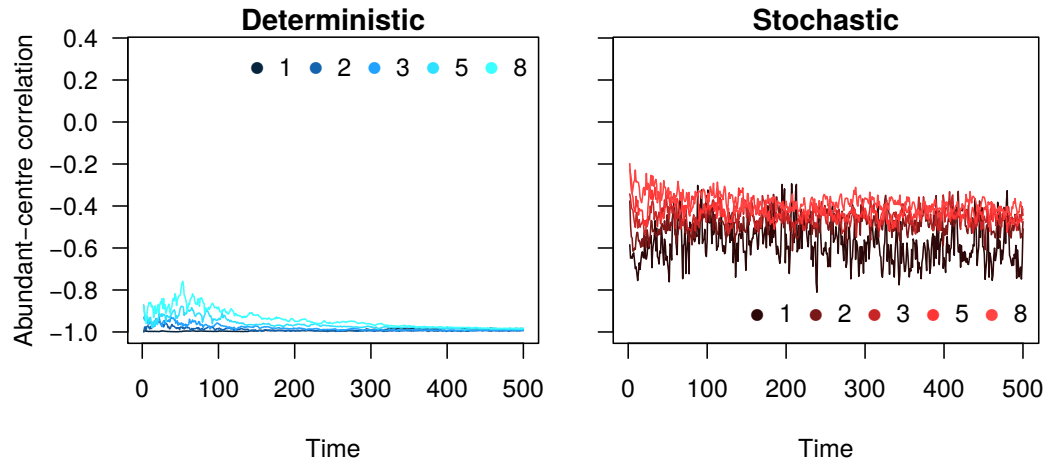


Figure A25. A representative simulation of abundant-centre relationships in climatic niche space – defined in a single dimension corresponding to population growth rates – the course of the 500 timestep simulation for both deterministic (left panel) and stochastic (right panel) model, examining the influence of step size  $\beta$ .

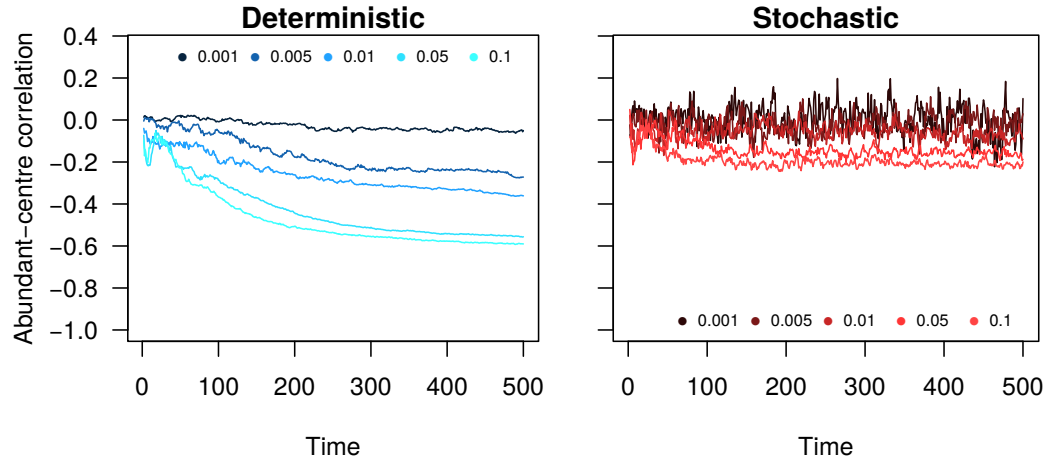


Figure A26. A representative simulation of abundant-centre relationships in climatic niche space – defined in a single dimension corresponding to population growth rates – the course of the 500 timestep simulation for both deterministic (left panel) and stochastic (right panel) model, examining the influence of dispersal probability  $P_d$ .